General Disclaimer

One or more of the Following Statements may affect this Document

- This document has been reproduced from the best copy furnished by the organizational source. It is being released in the interest of making available as much information as possible.

- This document may contain data, which exceeds the sheet parameters. It was furnished in this condition by the organizational source and is the best copy available.

- This document may contain tone-on-tone or color graphs, charts and/or pictures, which have been reproduced in black and white.

- This document is paginated as submitted by the original source.

- Portions of this document are not fully legible due to the historical nature of some of the material. However, it is the best reproduction available from the original submission.

cer

ATMOSPHERIC AND ENVIRONMENTAL RESEARCH, INC.
CAMBRIDGE, MASSACHUSETTS

OUTER SATELLITE ATMOSPHERES:
THEIR NATURE AND PLANETARY INTERACTIONS

Annual Report for Period
June 1, 1982 to May 31, 1983

Prepared for

NASA Headquarters
Washington, DC 20546

Prepared by

William H. Smyth
and
Michael R. Combi

Atmospheric and Environmental Research, Inc.
840 Memorial Drive
Cambridge, Massachusetts 02139

1. Report No.	2. Government Accession No.	3. Recipient's Catalog No.
4. Title and Subtitle Outer Satellite Atmospheres: Their Nature and Planetary Interactions		5. Report Date July 1983
		6. Performing Organization Code
7. Author(s) William H. Smyth and Michael R. Combi		8. Performing Organization Report No.
9. Performing Organization Name and Address Atmospheric and Environmental Research, Inc. 840 Memorial Drive Cambridge, Massachusetts 02139		10. Work Unit No.
		11. Contract or Grant No. NASW-3387
12. Sponsoring Agency Name and Address NASA Headquarters Headquarters Contract Division Washington, DC 20546		13. Type of Report and Period Covered Annual Report June 1, 1982– May 31, 1983
		14. Sponsoring Agency Code HWC-2

15. Supplementary Notes

16. Abstract

Significant progress is reported this year in early modeling analysis of observed sodium cloud images with our new model which includes the oscillating Io plasma torus ionization sink. Both the general 2-D morphology of the region B cloud as well as the large spatial gradient seen between the region A and B clouds are found to be consistent with an isotropic flux of $\sim 5 \times 10^8$ cm^{-2} s^{-1} of sodium atoms from Io. Model analysis of the spatially extended high velocity directional features has provided substantial evidence for a magneto-spheric wind driven gas escape mechanism from Io. In our efforts to define the source(s) of hydrogen atoms in the Saturn system, major steps have been taken in order to understand the role of Titan. We have completed the comparison of the Voyager UVS data with previous Titan model results, as well as the update of the old model computer code to handle the spatially varying ionization sink for H atoms.

17. Key Words (Selected by Author(s)) satellite atmospheres planetary magnetospheres comets	18. Distribution Statement

19. Security Classif. (of this report) Unclassified	20. Security Classif. (of this page) Unclassified	21. No. of Pages 30	22. Price*

*For sale by the Clearinghouse for Federal Scientific and Technical Information, Springfield, Virginia 22151.

TABLE OF CONTENTS

LIST OF FIGURES

LIST OF TABLES

I. INTRODUCTION

The progress achieved in the second year of this three-year research program is reported. The overall research program is organized into three different subjects: (1) the Jupiter system, (2) the Saturn system, and (3) Comets. In the Jupiter system, the extended atmospheres of Io and their relations and interactions with the planetary magnetosphere are the topic of interest. In the Saturn system, the hydrogen torus of Titan, the atmospheres associated with the planetary rings, and the extended atmospheres of the E-ring satellites are the topics of concern. For comets, the dust and gas clouds in the outer coma are the areas of focus.

The three primary goals of the overall program are (1) to better understand the characteristics of the local atmosphere of Io and the manner in which it interacts and delivers a significant source of heavy-ion plasma to the planetary magnetosphere, (2) to understand the spatial distribution of hydrogen in the Saturn system in terms of the planet, its rings and its satellite, and to better define the source of protons for the magnetosphere, and (3) to provide fresh insight into the chemical and physical nature of comets through study of their extended atmospheres. These research objectives are important in achieving better understanding of the basic satellite and magnetospheric processes in the outer solar system and basic comet and solar radiation processes in the inner solar system. To pursue these goals, the research program has employed both exploratory calculations to uncover important physical mechanisms and more-refined model calculations to evalute the quantitative significance of these mechanisms.

For the Jupiter system, the overall three-year research plan is summarized in Table 1. There are three major subjects. The first subject, the Io sodium cloud, is divided into five subtopics. Efforts during the second year have been focused primarily upon studying the 2-D intensity morphology and the directional features of the Io sodium cloud using our new model which incorporates the oscillation of the Io plasma torus about the satellite plane. ' Progress in these studies is discussed in Section II. Minor efforts have also been expended in initiating the development of the Io potassium cloud model using the appropriate information obtained in the first year of this program. This development, which is relatively straightforward, is to be completed in the third year and will not be discussed further in this report. The third

Table 1

JUPITER SYSTEM: THREE-YEAR PLAN FOR MODEL DEVELOPMENT AND ANALYSIS

Subject	First Year	Second Year	Third Year
Io Sodium Cloud Model Development	Update the model to include the oscillating Io plasma torus as an ionization sink (Phase 1) and simultaneously include the effects of solar radiation pressure (Phase 2)	Enhance CPU execution efficiency of the numerical model	-
(i) 2-D Intensity Morphology	-	Perform initial model calculations and compare with observed images of Murcray (1978) to determine the sodium atom flux and insight into the cloud structure	Perform model calculations to analyze the East-West asymmetries and the North-South alternating asymmetry of the cloud
(ii) Line Profiles	-	-	Perform model calculations for measured line profiles to study the satellite emission mechanism
(iii) Io Plasma Torus Interactions	Adopt a description of the electron density and temperature in the plasma torus and calculate the sodium electron impact ionization lifetime	Evaluate the effects of elastic ion-sodium collisions	Improve description of electron plasma data
(iv) Directional Features	Perform very preliminary one-orbit modeling analysis to roughly characterize the emission velocity of the features	Enhance model and analysis procedure. Perform initial model calculations to study the data of Pilcher (1982)	Perform additional model calculations to further refine insights into the emission mechanism
Io Potassium Cloud	Calculate the potassium electron impact ionization lifetime in the plasma torus. Obtain the solar spectrum for the two K emission intensity and acceleration produced by solar resonance scattering	Initiate development of the potassium cloud model by suitably modifying the sodium cloud model	Complete model development and perform model calculations appropriate to the observations of Trafton (1981)
Other Io Clouds	-	-	Provide exploratory modeling for newly discovered gas clouds

subject of Table 1 has remained inactive during the second year and will be activated in the third year in the event that new gas clouds (other than sulfur) are discovered. Exploratory modeling for the Io sulfur cloud (recently reported as detected by Durrance et al. 1983) is currently being pursued under a separate NASA contract.

For the Saturn system, the overall three year research plan is summarized in Table 2 and is organized into the study of four objects, each known or expected to provide a source of hydrogen atoms and ultimately protons to the circumplanetary space. During the second year, major emphasis has been placed upon better understanding the role of Titan (and ultimately non-Titan sources) in the new light that the planet may itself also provide a significant source of hydrogen to the Saturn system (Shemansky and Smith, 1982). Progress resulting from these efforts is discussed in Section III.

For Comets, research efforts have been mostly inactive in the second year and are scheduled to be activated in the third year. Cometary models developed at AER in previous NASA contracts will be refined in the third year of this research program and applied to comet coma observations.

Table 2

SATURN SYSTEM AND COMETS: THREE-YEAR PLAN FOR MODEL DEVELOPMENT AND ANALYSIS

Extended Atmosphere	First Year	Second Year	Third Year
Saturn System			
Planet	--	New Idea: The planet may be a source of H for the Saturn system (Shemansky and Smith, 1982) and may provide an alternate explanation for the ring atmosphere and part of the Titan H torus cloud	Further evaluate Saturn as an H source and, if warranted, develop a model for an extended H atmosphere for the planet
Saturn's Rings	Perform preliminary study for photo-sputtering of H₂0 ring-ice as an H source (problem too much oxygen remaining near rings)	--	Assess the importance of the rings as a source of gas for the Saturn system
E-Ring Satellites	--	Perform limited studies to ascertain the physical domain of H atoms for E-ring satellite sources	Assess the importance of the satellites as a source of gas for the Saturn system
Titan	--	Examine post-Voyager data for H atoms in the Saturn system Update pre-Voyager model to include a spatially dependent ionization of H in the Saturn magnetosphere	Complete the update of the Titan H torus model Perform model calculations and compare to the Voyager UVS data to ascertain the role of Titan as a source of H atoms
Comets	--	--	Complete model refinements Apply model to comet coma observations

ORIGINAL PAGE IS
OF POOR QUALITY

9

II. THE JUPITER SYSTEM: MODELING THE IO SODIUM CLOUD

2.1 Introduction

The three-year research plan for the Io sodium cloud in Table 1 is subdivided into general model development and four separate subtopics organized around the different types of observational data that are available. The second year of effort has been built upon the primary model-development activities of the first year and has focused upon an initial phase of model application for the subtopics (i) and (iv) of Table 1. The improved model, which now includes the oscillating Io plasma torus as a time-space varying sink for sodium (see Figure 1), provides a new and powerful modeling resource that has already allowed us to draw some significant conclusions from observational data for these two subtopics in the second year. These conclusions are discussed below. In addition, the computer code for the model has been improved in the second year by rearranging information inside of the CRAY 1 vector loops so that the cpu execution speed is now about 30% faster.

2.2 The Region B Cloud

The new sodium cloud model, that explicitly includes the oscillating plasma torus, has been used to calculate the two-dimensional intensity morphology of the brighter portion of the cloud (i.e., the Region B cloud) on the sky plane for several of the sodium cloud images obtained by Murcray (1978). One of these observed images at a satellite phase angle of 129° and a system III magnetic longitude of Io of 9° (based on the 1965 system in which the north pole is inclined toward 200°) is shown in Figure 2. A model calculation for these same conditions is shown in Figure 3.

In the model results in Figure 3, sodium atoms were emitted radially and isotropically from Io's exosphere (assumed 2600 km in radius) with an initial speed of 2.6 km sec^{-1} and with an assumed constant flux of 4.8×10^8 atoms cm^{-2} sec^{-1} (based upon the surface area of the satellite). The effects of solar radiation pressure (although included as an option in the model) were excluded in this calculation as a first step in evaluating the impact of the plasma torus on the cloud. These effects are expected to be first order corrections to the central conclusions to be drawn here and will be included in the exploratory calculations considered in the third year. In Figure 3, the overall shape and absolute D_2 intensity calculated for the cloud beyond the occulting
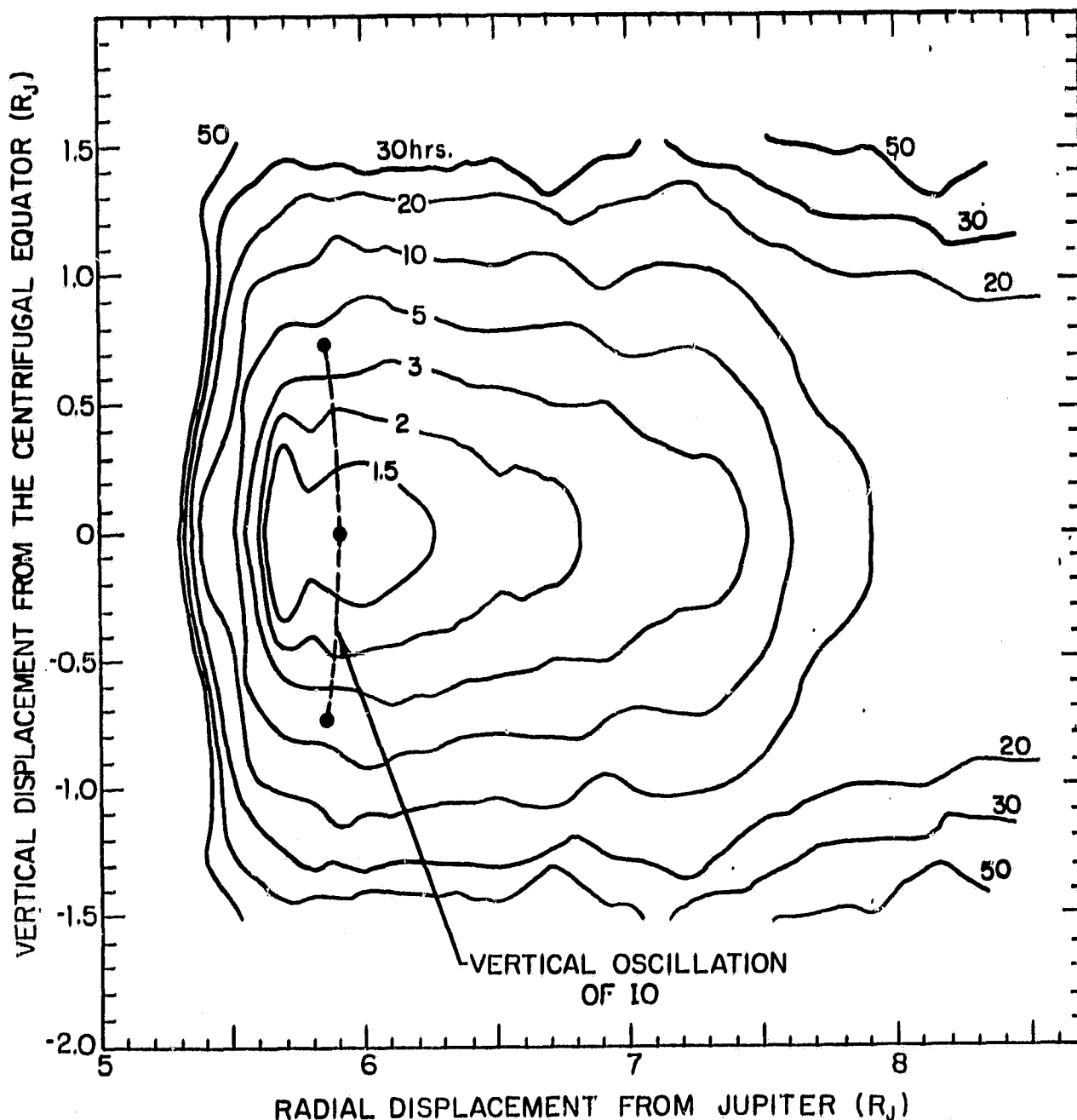
Figure 1: Sodium Electron Impact Ionization Lifetime in Io Plasma
Torus. The lifetime calculation is based upon the
measured cross-section by McFarland (1965), McFarland
and Kinney (1965) and Zapesochnyi and Aleksakhin (1968),
the Voyager 1 data for the plasma density (Bridge,
Sullivan and Bagenal, 1980; Bagenal and Sullivan,
1981) and for the electron temperature deduced from
the Voyager 1 UVS data (Shemansky, 1980) and in situ
measurements (Scudder, Sittler and Bridge, 1981).
The two-dimensional common temperature model of Bagenal
and Sullivan (1981), was selected to describe the electron
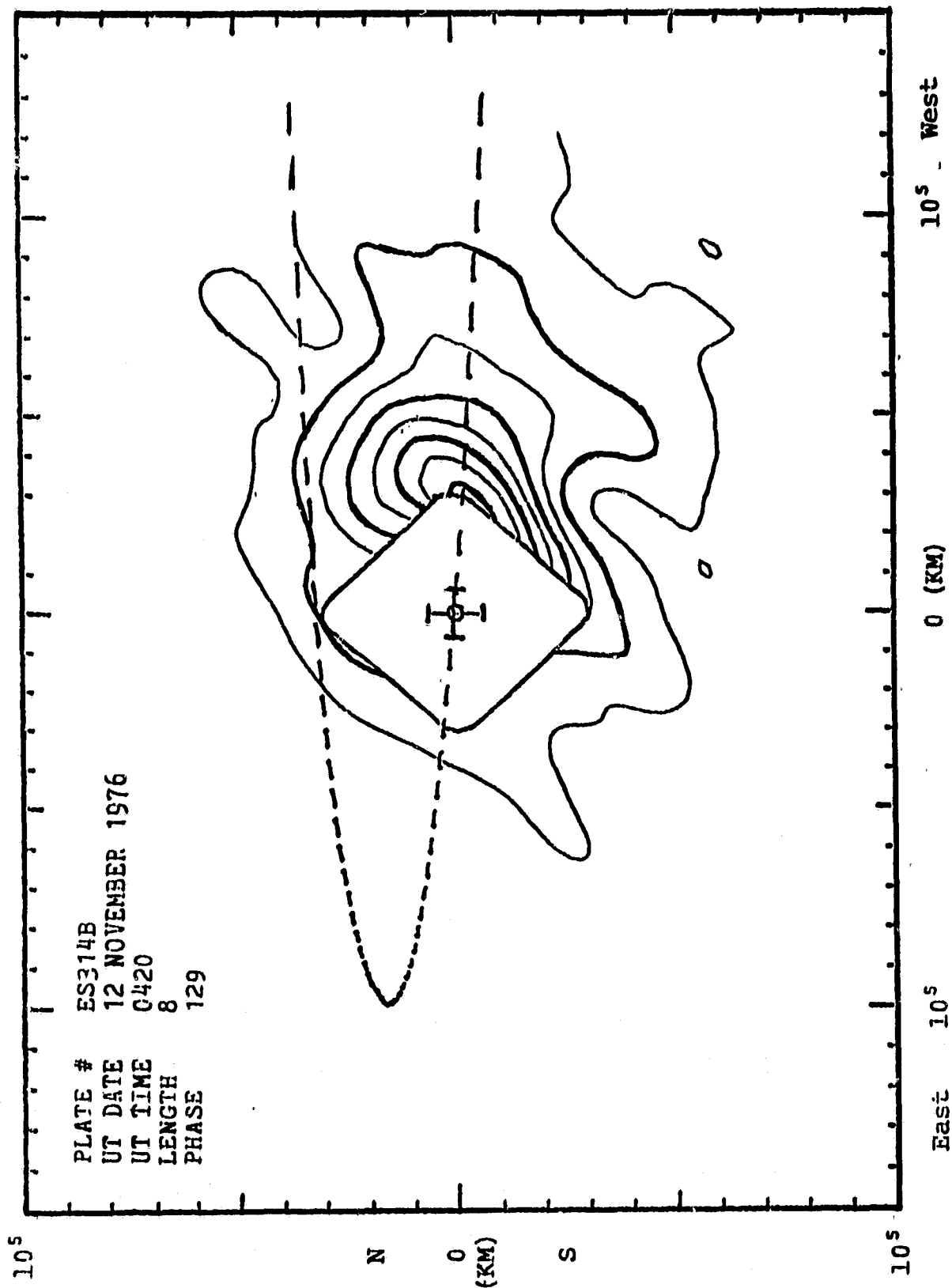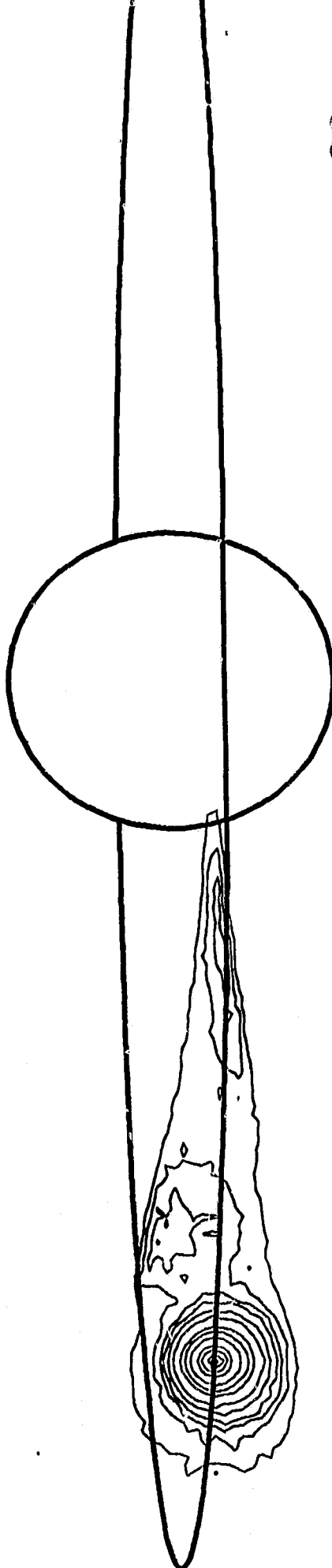density.

Figure 2. Io Sodium Cloud Image. The D₂ intensity image was measured in 1976 by Murcray. (1978) with a central rectangular mask covering Io and the brightest intensity near the satellite. The outer contour brightness is 0.5 kR (kilo Rayleigh) with contours increasing inward by 0.5 kR steps. Io's orbit projected onto the sky plane is shown by the dashed line.

SODIUM D2 LINE INTENSITY

Figure 3. Model Calculation for the Io Sodium Cloud. The model calculated D_2 intensity of the Io sodium cloud corresponding to the observation of Figure 1 is shown. Model parameters used are given in the text. Brightness contour levels are given in kR and have values from the outer to the inner contour of 0.5, 1.0, 1.5, 2.0, 3.0, 5.0, 10.0, 15.0, 25.0, 50.0, 75.0, and 100.0.

mask are similar to the observed image in Figure 2. Behind the occulting mask in Figure 3, the cloud intensity increases with decreasing distance from Io by almost two orders of magnitude. This sharp gradient in the cloud intensity is consistent with the large integrated D_2 intensity values measured by Bergstralh et al. (1975, 1977) through a 3 x 8 arc sec reactangular aperture centered on Io and with unpublished values of the D_2 intensity in a 9 arc sec diameter circle centered on Io measured more recently by Goldberg (1982). This result is particularly gratifying and provides a natural solution to our earlier non-oscillating torus modeling results [see: NASA Final Report for Period February 1979 to March 1980, page 46] where the central intensity near Io was much too large. The oscillating of the plasma torus, as expected from Figure 1, reduces the effective strength of the sink more for atom trajectories that populate the forward cloud (i.e., atom trajectories inside of Io's orbit and also inside of the ionization sink of the plasma torus) than for atom trajectories that move outside and behind Io's orbit.

Further comparisons of model calculations with other observed images of Murcray also provide similar results to that of Figures 1 and 2, so that three very important conclusions may be drawn:

(1) The presence (at non-critical Io phase angles) of a predomi-nantly forward sodium cloud and the absence of a predomi-nantly trailing sodium cloud is consistent with an isotropic emission of sodium from Io and the radial structure of an oscillating plasma torus which produces a very asymmetric electron-impact ionization sink for sodium (see Figure 1).

(2) The length of the forward sodium cloud is determined natur-ally by the plasma torus and occurs when the orbital paths of sodium atoms in the forward cloud have their second ioniza-tion encounters with the plasma torus somewhat ahead of Io (see Figure 4, which also illustrates how the forward cloud length is expected to be further altered by the effects of solar radiation pressure).

(3) The flux of sodium from Io necessary to produce the measured two-dimensional intensity morphology of the B-cloud and also the much larger intensity values very near Io is approxim-ately 5 x 10^8 atoms cm^{-2} sec^{-1}, (i.e., a total source of about 2 x 10^{26} atoms sec^{-1}, with a more refined value to be
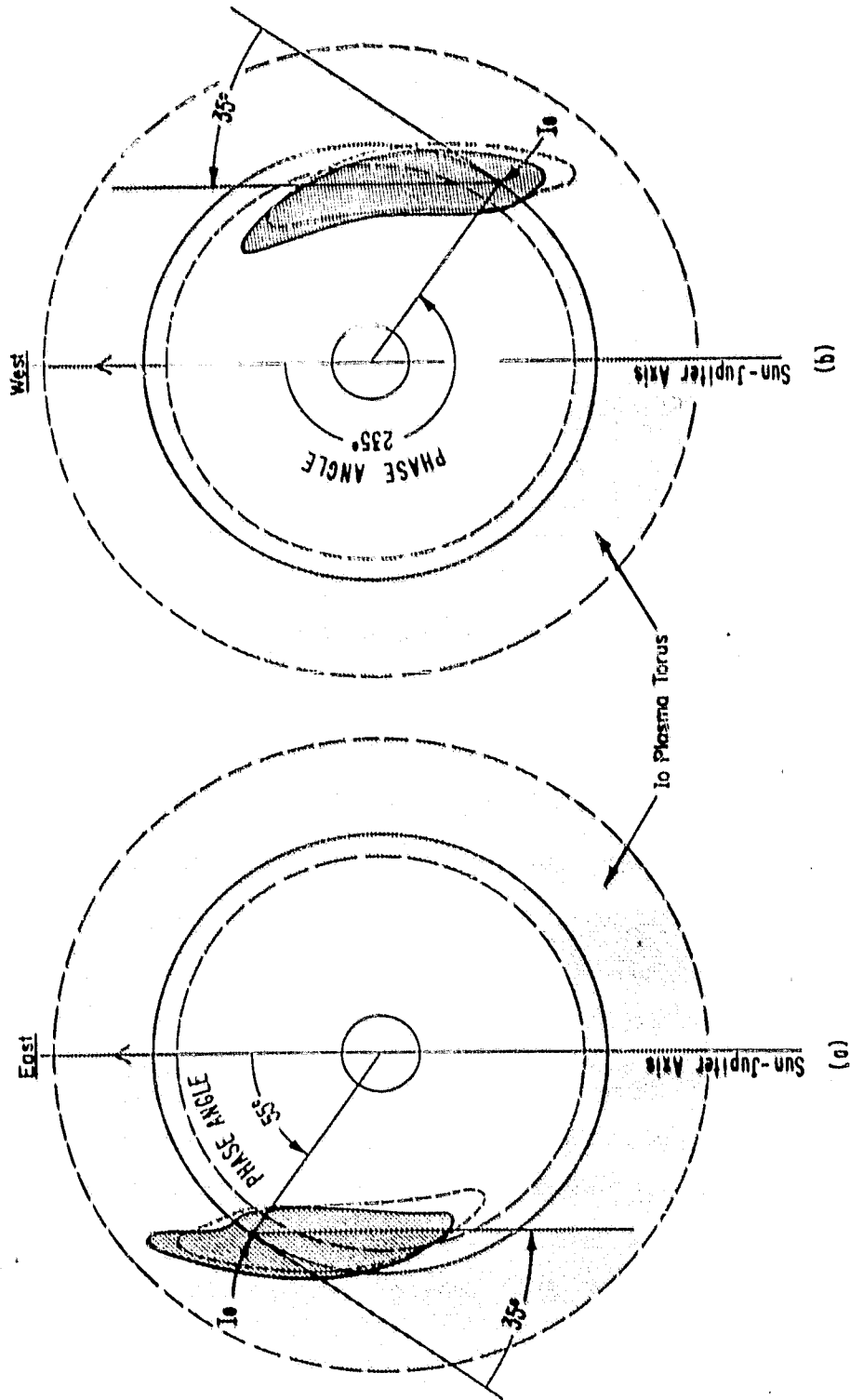
Figure 4. Interaction of the Sodium Cloud and the Plasma Torus. The spatially-projected overlap in the satellite plane of the Io plasma torus with the solar radiation perturbed cloud shape (solid boundary with heavy shading) and with the unperturbed cloud shape (heavy dashed boundary) is indicated for the diametrically opposite satellite phase angles. The cloud shape illustrates the envelope of sodium atoms after 20 hours of flight time.

achieved when a more explicit description of the initial exo-
spheric velocity dispersion is deduced or otherwise
measured).

Comparisons of additional model calculations with the observational data of
Murcray (1978) and with more recently acquired but unpublished data of Goldberg
(1983, with whom a collaborative effort has recently been established) are
required to address the more refined features of the region B cloud, such as
the east-west asymmetries (Bergstralh et al. 1975, 1977; Smyth, 1979; Goldberg
et al. 1980; Goldberg 1981; Smyth, 1983) and the north-south alternating asym-
metry (Trafton and Macy, 1975; Trafton 1977, 1980), and other small scale
changes that may appear in the cloud as the result of the oscillation of the Io
plasma torus about the satellite plane. Such comparisons will provide informa-
tion about the initial velocity distribution of sodium atoms emitted by Io and
the nature of the local satellite atmosphere.

2.3 Interaction with the Io Plasma Torus

Ions and electrons in the Io plasma torus may interact with the sodium
cloud in two ways. First, the plasma torus determines the lifetime of sodium
atoms through the inelastic collisional processes of either electron impact
ionization (as illustrated in Figure 1) or charge exchange reactions with heavy
ions. Second, the heavy ions in the plasma torus may provide a non-gravita-
tional acceleration for some cloud atoms through elastic collisions. Relevant
inelastic and elastic reactions for sodium in the plasma torus are summarized,
together with the sodium atom reaction time, in Table 3. The electron-impact-
ionization reaction time is a minimum value and is taken from Figure 1. Cross
sections used to compute the charge-exchange reaction times were obtained from
Johnson and Strobel (1982) and Rutherford et al. (1972). Reaction times for
the elastic ion-neutral collisions were taken from Brown, Pilcher and Strobel
(1983).

From Table 3, the lifetime of sodium atoms in the Io plasma torus can be
seen to be dominated by electron impact ionization. Inside of about 5.5
Jupiter radii, where the electrons become too cool to ionize sodium (see Figure
1), the dominant plasma torus ions (O^+ and S^+) have very small cross sections
and are incapable of modifying the sodium abundance. Only the effects of elas-
tic collisions (with reaction time $\geq$ 60 hours) and charge exchange with Na^+
(with reaction time $\sim$ 50 hours) are capable of modifying the sodium abundance

Table 3

Reactions for Sodium Atoms in the Io Plasma Torus

Reaction	Sodium Atom Reaction Time (hr)
1. $e + Na \rightarrow Na^+ + 2e$	~1
2. $O^+ + Na \rightarrow O + Na^+$	∞
3. $S^+ + Na \rightarrow S + Na^+$	∞
4. $Na^+ + Na \rightarrow Na + Na^+$	~50[a]
5. $O^{++} + Na \rightarrow O^+ + Na^+$	~30[b]
6. $S^{++} + Na \rightarrow S^+ + Na^+$	~20[b]
7. $h\nu + Na \rightarrow Na^+ + e$	~400
8. $X^+ + Na \rightarrow X^+ + Na$ (elastic collision)	~20-60[c]

[a] Assumed a nominal ion density of 50 cm^{-3} (i.e., ~5% abundance) and a 60 km sec^{-1} ion-neutral velocity

[b] Assumed a nominal density of 10^3 cm^{-3} and a 60 km sec^{-1} ion-neutral velocity

[c] Assumed values between 1000 and 3000 positive charges cm^{-3}

in this region and these reactions are limited vertically to within about 0.1 to 0.2 Jupiter radii of the centrifugal equator because of the cold ion temperature. For the region-B cloud, which resides significantly inside of Io's orbit for a time of order 20 hours (see Figure 4), the effects of the plasma torus on the sodium cloud abundance inside of 5.5 Jupiter radii should be small. The lifetime of sodium determined by electron impact (see Figure 1) is therefore the only collisional process in the plasma torus that is required to model the sodium abundance realistically. Ion-neutral collisional interactions of the plasma with the satellite surface and its local atmosphere appear to be important, however, as is evident in the discussion of the directional features in the next section.

2.4   The Directional Features

The new sodium cloud model has also been used to study the directional features of the sodium cloud discovered by Pilcher (see Hartline, 1980) in data taken at the Mauna Kea Observatory in 1980 and 1981. To understand these features, a collaborative effort with Pilcher has been in progress during the last two years. During the past year, the basic idea under evaluation has been to determine if the directional features, observed outside of Io's orbit on the sky plane, could be understood in terms of a high velocity ($\sim$20 km sec^{-1}) source and the time-varying sodium sink produced (through electron-impact ionization) by the plasma torus as it oscillates about the satellite plane.

To investigate this idea a correlation analysis procedure was devised and implemented to analyze the relationship between the model-calculated, time-varying D-line intensity probability on the sky plane and the vector orientation of sodium atoms emitted from Io. This procedure was then applied to study several sky plane images of the directional features supplied to us by Pilcher. These images showed that the features appearing on the sky plane outside of Io's orbit could change their direction from south to north of the satellite plane in a period of several hours. The results of applying our correlation procedure to these images was to show that to produce a feature that changes its direction from south to north with the observed value of the Io magnetic longitude, the atom emission velocities from Io would be required to have some limited angular dispersion that is approximately centered at right angles to the direction of motion of the satellite. This direction of emission velocities is the same as determined by Dr. Robert E. Johnson (University of

Virginia) and his graduate student Edward Sieveka (Johnson and Sieveka, 1982) who have shown, through elastic collisional calculations for moving ions and stationary sodium atoms, that sodium is preferentially scattered at nearly right angles to the ion flow direction.

Model calculations performed near the end of this second program year have confirmed the results of our earlier correlational analysis. From this we conclude that the directional features provide substantial support for a satellite gas escape mechanism that is driven by the planetary magnetospheric wind as it flows around Io. The results of this analysis are far reaching and will be reported in a paper to be completed early in the third year of this program. These results will also be reported at IAU Colloquium No. 77, "Natural Satellites" (Pilcher, Smyth and Combi, 1983).

III. THE SATURN SYSTEM: UNDERSTANDING THE DISTRIBUTION OF H-ATOMS

3.1 Introduction

For the Saturn system, a condensed summary of our three year research program is given in Table 2. Of the four subtopics listed in Table 2, the Titan hydrogen torus has been a long-standing topic at AER (Smyth, 1981) which was supported by NASA several years before this current program began. Efforts at AER to understand the extended ring and E-ring satellite atmospheres were initiated in 1980-81, one year before the current program began. For this reason, efforts in the first year of this research program (see Table 2) were directed primarily to the planetary ring atmosphere, where new data had become available from the Voyager 1 and Voyager 2 encounters. In the second year of this program, however, the planet was recognized as being a possible source of H for the larger Saturn system (Shemansky and Smith, 1982) and the scope of the problem has been appropriately broadened and refocused as indicated by the addition of the fourth topic in Table 2. An extended hydrogen atmosphere for Saturn must now be considered as a plausible source of H atoms previously interpreted as a planetary ring atmosphere and might even be an important source for some of the hydrogen previously associated with a Titan source.

At present, therefore, there appear to be four likely sources to supply the neutral hydrogen distribution observed in Saturn's magnetosphere. To further explore and understand this subject, our past collaborative effort with D. E. Shemansky (regarding the Titan torus data obtained by the UVS instrument of the Voyager spacecrafts) has been expanded in scope this year. The first step in the expanded collaboration with Shemansky has been to begin to update the Titan model to include the lifetime processes (electron impact ionization, charge exchange, and photoionization) for hydrogen operative in Saturn's magnetosphere. Model calculations of the Lyman-α intensity in the magnetosphere produced by H atom loss by Titan may then be properly calculated and compared to the UVS measurements of the Voyager spacecraft. By studying differences in these calculated and measured intensities, the importance of non-Titan gas sources may be assessed. Such analysis may allow us to determine, for example, if gases from the E-ring satellites Tethys and Dione (for which spatial gas envelopes are illustrated in Figure 5) are relevant in understanding the Voyager UVS data. Specific efforts in the second year to improve the Titan hydrogen torus model are discussed below.
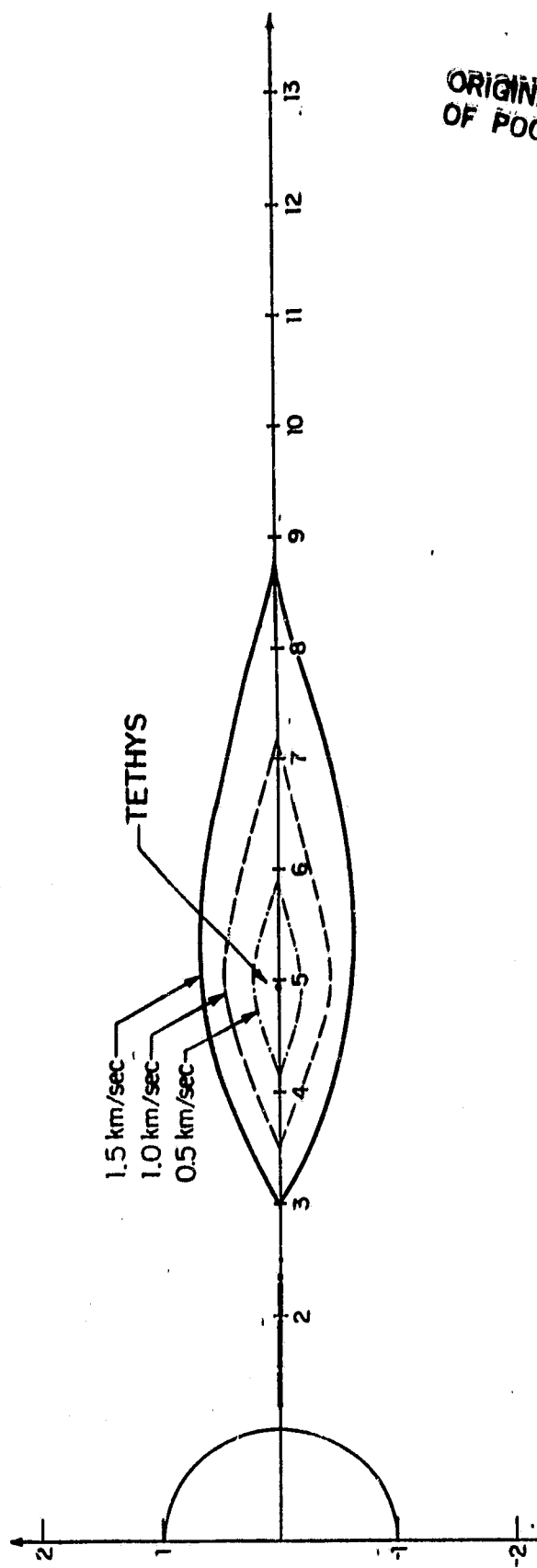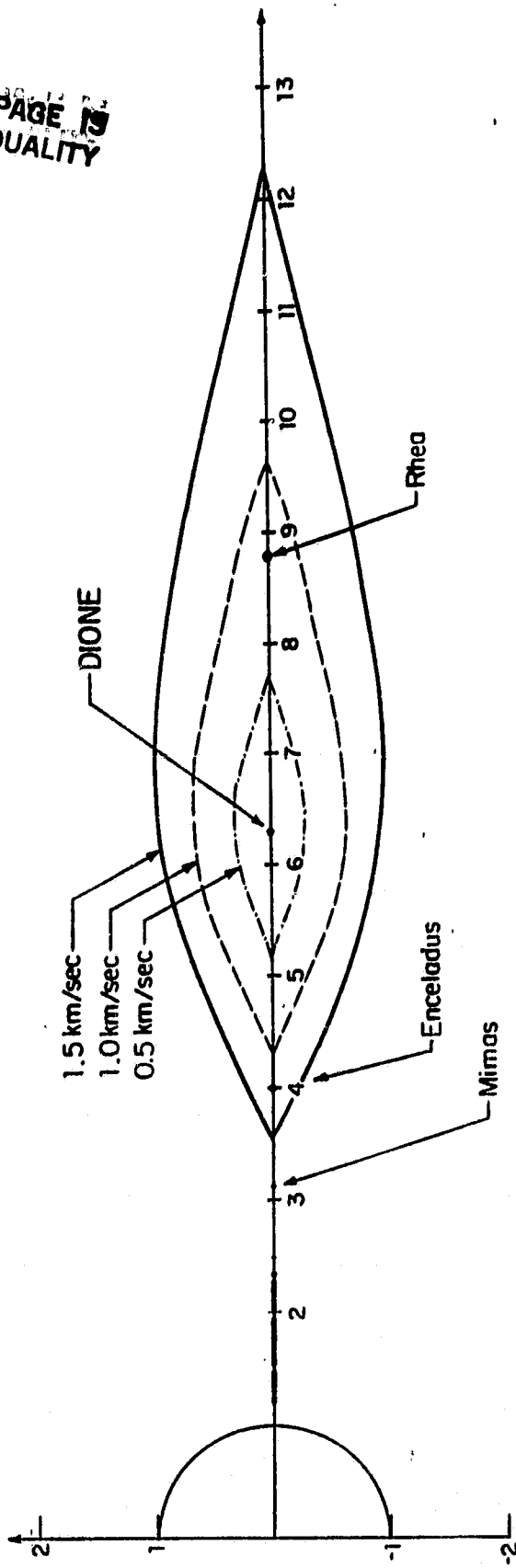
Figure 5. Spatial Envelopes for Neutral Gas Clouds of Tethys and Dione. The spatial envelope that contains gas atoms emitted from the satellite with velocities of 0.5, 1.0 and 1.5 km/sec. is shown in relation to Saturn, the main planetary rings and other E-ring satellites.

21

3.2 The Role of Titan

Efforts in the past year toward understanding the role of Titan in the production of Saturn's hydrogen torus have centered around (1) comparing the previous modeling work done at AER (Smyth, 1981) with Voyager 1 and Voyager 2 data, (2) gathering the information necessary to specify the plasma conditions operative at Saturn so the spatial dependence of the hydrogen lifetime can be properly modeled, and (3) updating the previous Titan hydrogen model computer code to include the spatially varying sink. Progress in this areas has been recently reported at the Fifth Conference on the Physics of the Jovian and Saturnian Magnetospheres (Combi and Smyth, 1983).

Figure 6 shows the previously modeled Lyman α distribution on the sky plane from a Titan hydrogen source with a flux of 3×10^9 cm^{-2} sec^{-1} from an exosphere of 5000 km radius and an ejection velocity of 2 km sec^{-1} (Smyth, 1981). A constant lifetime of 2×10^7 sec had been assumed for hydrogen atoms. Based on the results of the Plasma Science experiment on Voyager 2, Bridge et al. (1981) calculated the radial dependence in the equatorial plane of the hydrogen lifetime. The calculations included electron impact ionization, charge exchange, and photoionization processes. Figure 7 compares the spatially dependent lifetime with that used in the model. Although scale height effects will cause the lifetime to increase with distance from the equator, the major effect of this type of lifetime structure will deplete hydrogen originating at Titan inside of 10 Saturn radii (R_S) as compared with the model run.

The principal direct observational data which can be compared with the model come from the Ultraviolet Spectrometers (UVS) on board Voyager 1 and Voyager 2. The Voyager 1 UVS scanned the hydrogen torus along the equatorial plane in the light of Lyman α. Broadfoot et al. (1981) concluded that a uniform distribution of hydrogen (10 cm^{-3}) in a cylindrical torus from 8 to 25 R_S in radius and at least 6 R_S in height could reproduce the scan data. Figure 8 shows the UVS scan compared with a similar scan recently produced from the original model results. Note that in the model scan the Titan source can be directly seen at eastern elongation; also note that there is a definite enhancement at Titan's orbital distance (20 R_S) even at western elongation. This enhancement is not clearly seen in the UVS data. In the UVS data, Titan's location around Saturn is not fixed at eastern elongation, but has an angular distribution around the planet that has not yet been determined from the data

ORIGINAL PAGE IS
OF POOR QUALITY

TITAN 5600 hr.

Max. Signal = 434 Rayleighs
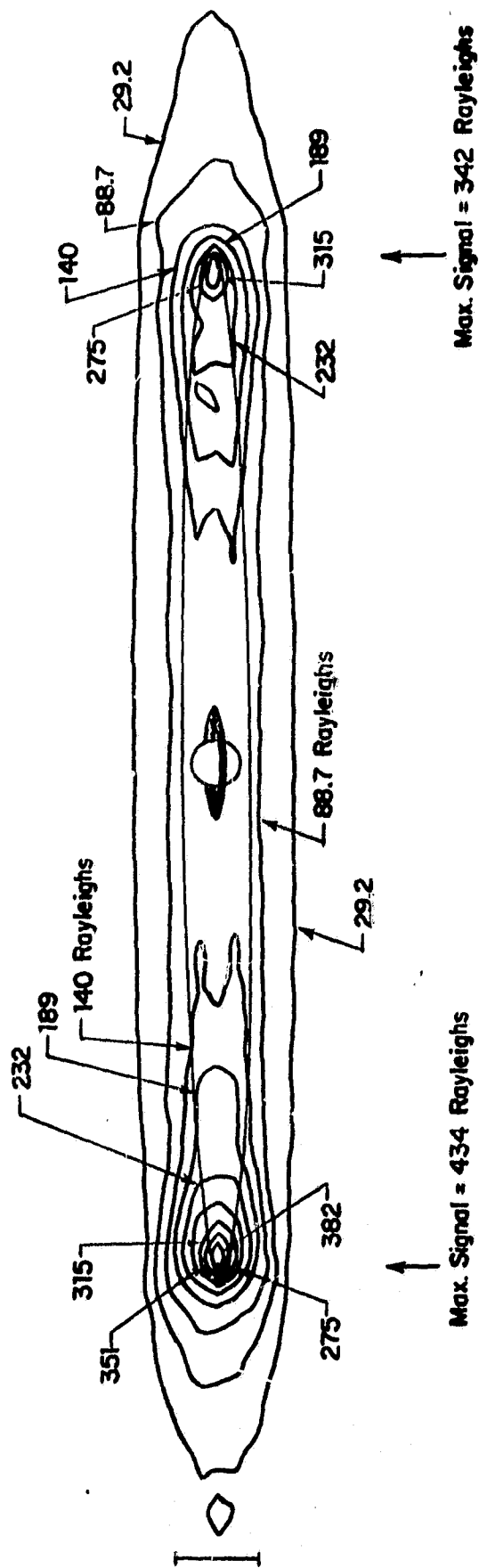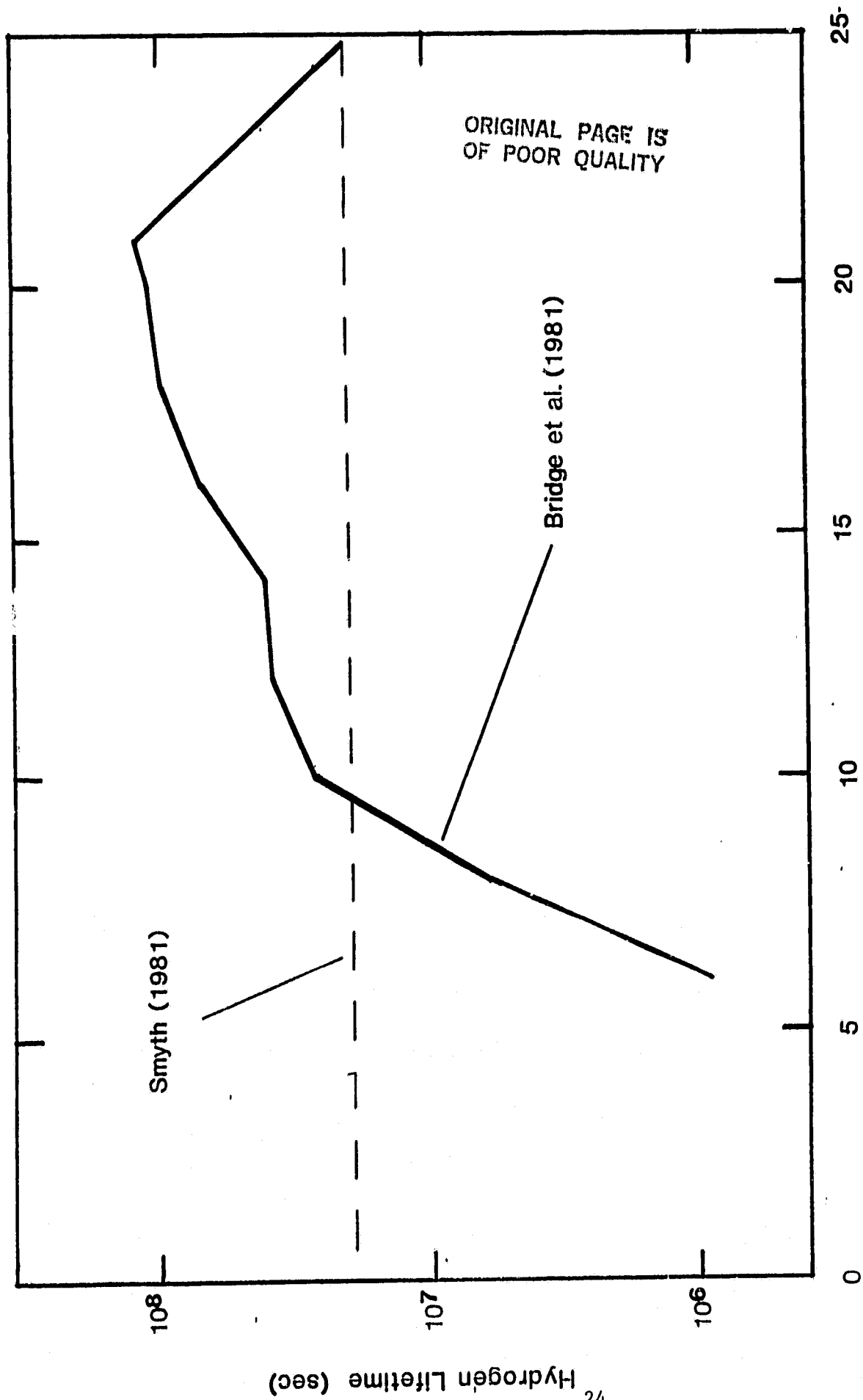
Max. Signal = 342 Rayleighs

Figure 6. Model Calculation of Lyman α Emission from the Titan Hydrogen Torus. Intensity contours, calculated assuming resonance scattering of sunlight, are shown for the satellite plane tilted by 3.25°. An isotropic emission of H atoms with an initial speed of 2.0 km s^{-1}, a satellite flux of 3 × 10^9 cm^{-2} s^{-1} and the indicated lifetime were assumed.

Figure 7. Radial Dependence of the Hydrogen Lifetime in the Equatorial Plane. The dashed line corresponds to the constant value resumed in the model of Smyth (1981). The solid curve is the lifetime calculated by Bridge et al. (1981) from the Voyager 1 PLS data.
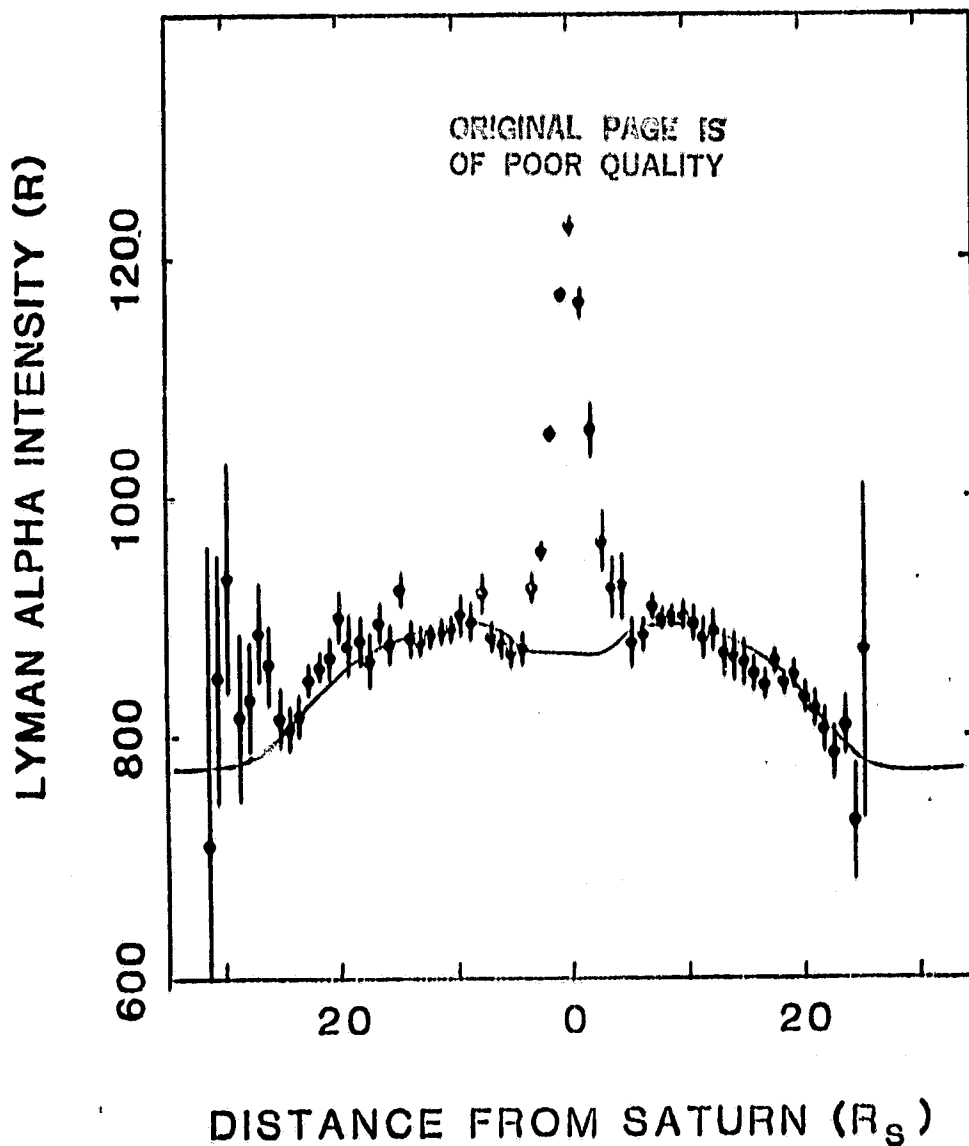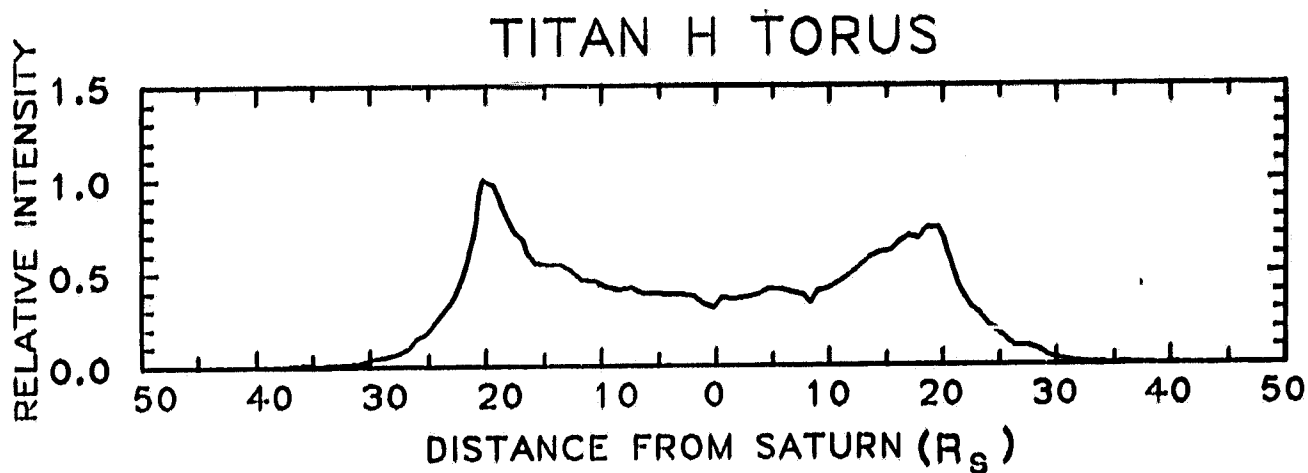
24

TITAN H TORUS

Figure 8. Model vs. UVS Lyman α Scan of the Hydrogen Torus. Below is the Voyager 1 UVS Lyman α scan, the solid line is the simple constant density torus discussed in the text. The central peak in the data points is due to the convolution of Saturn's Lyman α disk by the UVS slit. Above is the corresponding scan produced from the original model by Smyth (1981) for a Titan produced Hydrogen Torus.

set. Another difference in Figure 8 between the data and model is the decrease in brightness moving in from 20 R_S in the model but the continued increase in brightness in the data all the way to 8 R_S.

A slightly different comparison is shown in Figure 9. This shows the number of hydrogen atoms per .1 R_S cylindrical shell as a function of radial distance in the equator for both the Titan model and the simple UVS constant density model. The underestimation of the hydrogen abundance from 8 to 13 R_S in the model can be clearly seen.

Sandel et al. (1982) reported the Voyager 2 UVS Lyman α scan perpendicular to the equatorial plane which showed that the hydrogen torus extends to 6-8 R_S above and below the equatorial plane. This would require a Titan hydrogen source velocity of 2.6 km s^{-1} from its exosphere which is also consistent with the temperature of 186 K reported by Smith et al. (1982) for Titan's exosphere. This higher initial velocity would also populate radial distances within 6 R_S from Saturn.

The question left unanswered at this point is whether the increased velocity implied by the Voyager 2 data will increase the hydrogen density inside 10 R_S enough to offset the effects of a severe sink implied in this region by the plasma conditions. If the sink is too strong, it may be necessary to consider a source or sources in addition to or instead of Titan for Saturn's hydrogen torus.

In order to answer this question it is necessary to describe quantitatively the spatial dependence of the hydrogen lifetime in two dimensions: the radial distance from Saturn in the equator and the vertical displacement from the equator. This effort in collaboration with D. E. Shemansky was discussed in the previous section. Some preliminary but as yet incomplete plasma data have been obtained from the Voyager PLS team (McNutt, 1983) in this regard.

Finally, the structure of the previous Titan hydrogen model computer code has already been successfully updated to include the two-dimensional lifetime structure, once the data are available. At that point only the correct lifetime data needs to be added in order to completely update the code.
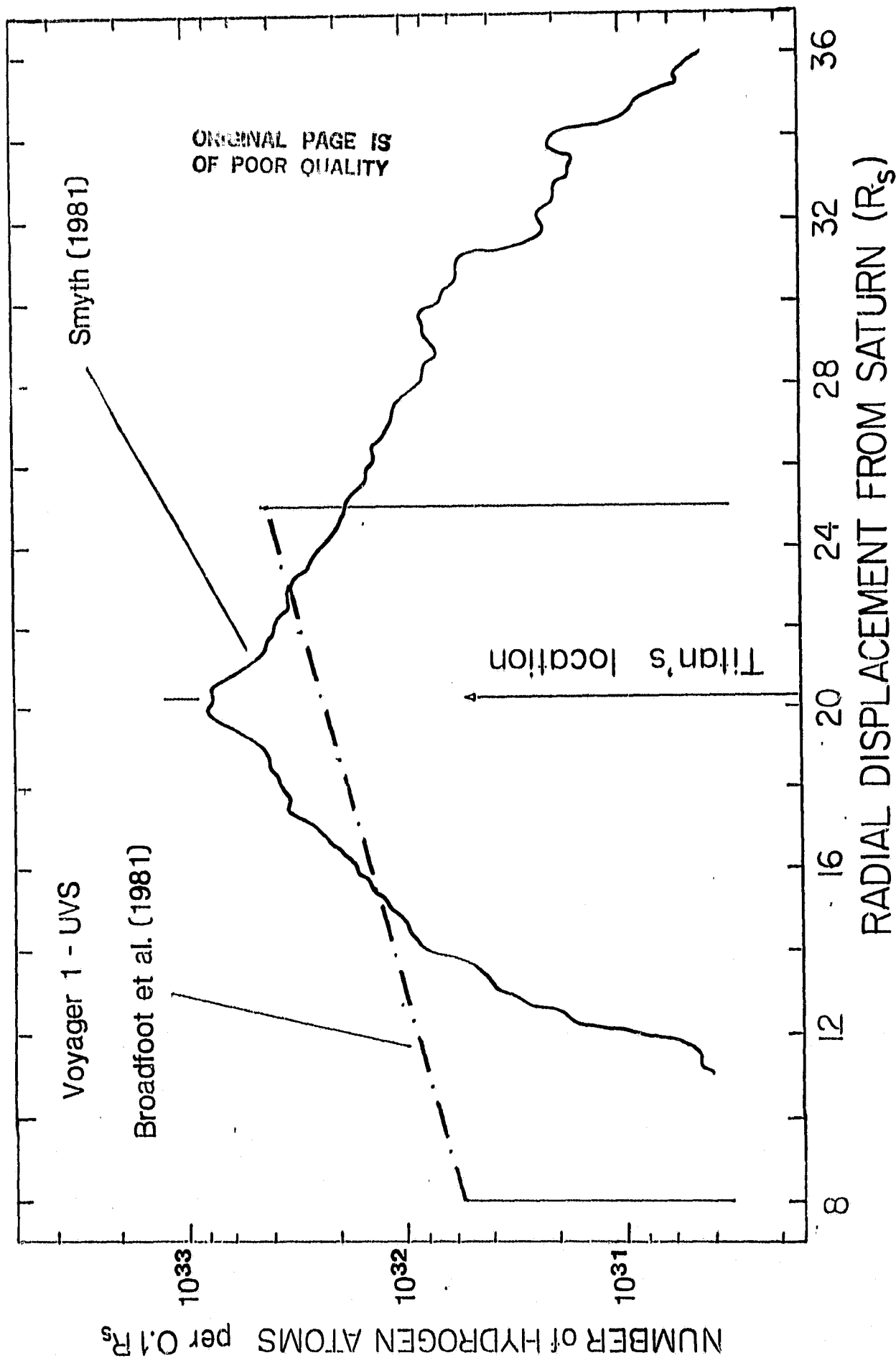
Figure 9. Radial Distribution of Hydrogen in the Torus. The solid line is from the model calculation of Smyth (1981). The dashed line represents the simple constant density distribution used by Broadfoot et al. (1981) to fit the Voyager 1 UVS Lyman α data.

IV. REFERENCES

Bagenal, F. and J.D. Sullivan (1981) Direct Plasma Measurements in the Io Torus and Inner Magnetosphere of Jupiter. J. Geophys. Res., 86, 8477.

Bergstralh, J.T., D.L. Matson and T.V. Johnson (1975) Sodium D-Line Emission from Io: Synoptic Observations from Table Mountain Observatory. Ap. J. Lett., 195, L131.

Bergstralh, J.T., J.W. Young, D.L. Matson and T.V. Johnson (1977) Sodium D-Line Emission from Io: A Second Year of Synoptic Observations from Table Mountain Observatory. Ap. J. Lett., 211, L51.

Bridge, H.S., J.D. Sullivan and F. Bagenal (1980) Private Communication.

Bridge, H.S. et al. (1981) Plasma Observations Near Saturn: Preliminary Results from Voyager 2. Science, 205, 208.

Broadfoot, A.L. et al. (1981) Extreme Ultraviolet Observations from Voyager 1 Encounter with Saturn. Science, 212, 206.

Brown, R.A., C.B. Pilcher and D.F. Strobel (1983) Spectrophotometric Studies of the Io Torus. in Physics of the Jovian Magnetosphere, A.J. Dessler (ed.), Cambridge University Press, NY.

Combi, M.R. and W.H. Smyth (1983) H and H$^+$ in Saturn's System: Understanding the Role of Titan. Paper presented at the Fifth Conference on the Physics of the Jovian and Saturnian Magnetospheres, June 22, Massachusetts Institute of Technology, Cambridge, MA.

Durrance, S.T., P.D. Feldman and H.A. Weaver (1983) Rocket Detection of Ultraviolet Emission from Neutral Oxygen and Sulfur in the Io Torus. Ap. J. Lett., 267, L125-L129.

Goldberg, B.A. (1981) Private Communication.

Goldberg, B.A. (1982) Private Communication.

Goldberg, B.A. (1983) Private Communication.

Goldberg, B.A., Yu Mekler, R.W. Carlson, T.V. Johnson and D.L. Matson (1980) Io's Sodium Emission Cloud and the Voyager 1 Encounter. Icarus, 44, 305.

Hartline, B.K. (1980) Voyager Beguiled by Jovian Carrousel. Science, 208, 384.

Johnson, D.E. and E.M. Sieveka (1982) Private communication.

Johnson, R.E. and D.F. Strobel (1982) Charge Exchange in the Io Torus and Exosphere. J. Geophys. Res., 87, 10,385.

McFarland, R.H. (1965) Phys. Rev., 139, A40.

McFarland, R.H. and J.D. Kinney (1965) Phys. Rev., 137, A1058.

McNutt, R.L. (1983) Private Communication.

Murcray, F.J. (1978) Observations of Io's Sodium Cloud. Ph.D. Thesis, Dept. of
    Physics, Harvard University, January 1978.

Pilcher, C.B. (1982) Private communication.

Pilcher, C.B., W.H. Smyth and M.R. Combi (1983) Io's Sodium Directional
    Features: Direct Evidence for a Magnetospheric-Driven Gas Escape
    Mechanism. Paper presented at IAU Colloquium No. 77, "Natural
    Satellites", July 7, Cornell University, Ithica, NY.

Rutherford, J.A., R.F. Mathis, B.R. Turner and D.A. Vroom (1972) Formation of
    Sodium Ions by Charge Exchange. J. Chem. Phys., 56, 4654.

Sandel, B.R. et al. (1982) Extreme Ultraviolet Observations from the Voyager 2
    Encounter with Saturn. Science, 215, 548.

Scudder, J.D., E.C. Sittler, Jr. and H.S. Bridge, (1981) A Survey of the Plasma
    Electron Environment of Jupiter: A View from Voyager. J. Geophys. Res.,
    86, 8157.

Shemansky, D.E. (1980) Private Communication.

Shemansky, D.E. and G.R. Smith (1982) Whence Comes the "Titan" Hydrogen
    Torus? EOS, 63, 1019.

Smith, G.R. et al. (1982) Titan's Upper Atmosphere: Composition and Tempera-
    ture from the EUV Solar Occultation Results, JGR, 87, No. A3, 1351.

Smyth, W.H. (1979) Io's Sodium Cloud: Explanation of the East-West Asym-
    metries. Ap. J., 234, 1148.

Smyth, W.H. (1981) Titan's Hydrogen Torus. Ap. J., 246, 344.

Smyth, W.H. (1983) Io's Sodium Cloud: Explanation of the East-West
    Asymmetries. II. Ap. J., 246, 708.

Trafton, L. (1977) Periodic Variations in Io's Sodium and Potassium Clouds.
    Ap. J., 215, 960.

Trafton, L. (1980) An Explanation for the Alternating North-South Asymmetry of
    Io's Sodium Cloud. Icarus, 44, 318.

Trafton, L. (1981) A Survey of Io's Potassium Cloud. Ap. J., 247, 1125.

Trafton, L. and W. Macy, Jr. (1975) An Oscillating Asymmetry of Io's Sodium
    Emission Cloud. Ap. J. Lett., 202, L155.

Zapesochnyi, I.P. and I.S. Aleksakhin (1968) Zh. Eksp. Teor. Fiz., 55, 76
    [also, Soviet Physics, JETP, 28, 41 (1969)].